Available online at www.sciencedirect.com
ScienceDirect
Catalysis Today 133–135 (2008) 42–48
CATALYSIS TODAY
www.elsevier.com/locate/cattod

Preparation and characterization of Co mordenite coatings onto cordierite monoliths as structured catalysts

M.A. Ulla [b,*], R. Mallada [a], L.B. Gutierrez [b], L. Casado [a], J.P. Bortolozzi [b], E.E. Miró [b], J. Santamaría [a,*]

[a] Departamento de Ingeniería Química, Universidad de Zaragoza, Pedro Cerbuna 12, 50009 Zaragoza, Spain
[b] Instituto de Investigaciones en Catálisis y Petroquímica-INCAPE-(FIQ,UNL-CONICET), Santiago del Estero 2829, 3000 Santa Fe, Argentina

Available online 14 January 2008

Abstract

Mordenite coatings onto the walls of cordierite monoliths were obtained by hydrothermal synthesis followed by cationic exchange. A battery of characterization techniques was used to describe the structured catalyst so obtained, and selective catalytic reduction (SCR) of NO with CH_4 in excess O_2 was used as a reaction test. A homogeneous distribution of the different components on the synthesized mordenite layer was obtained, with a Si/Al ratio lower than that of synthesis gel, suggesting aluminium transference from the substrate to the zeolite during the synthesis procedure; however, this effect was not observed for Mg. TPR results indicated that Co species in mordenite were exchanged Co^{2+}, highly dispersed CoO_x, and hydroxo-Co with a small contribution of Co_3O_4. The existence of different Co^{2+} sites is supported by NO desorption tests. Catalytic performance was fairly comparable to that of powdered Co-mordenite.

Keywords: Mordenite coating; Structured catalyst; NO-SCR

1. Introduction

The importance of zeolites as catalysts and adsorbents is well known [1], due to their characteristic properties: high specific surface areas, well-defined microporous structures and the presence of exchangeable cationic sites (whose density relates to the Si/Al ratio of the structure), among others.

These aluminosilicates are obtained by hydrothermal synthesis that in general produce particles with reduced sizes (tens to hundreds of microns). For many catalytic applications (such as fixed bed and slurry reactors) these small particle sizes give rise to a variety of problems (large pressure drop in fixed beds, catalyst separation in slurry and entrained reactors, etc. [2]), prompting the use of different contactors. One of the most successful alternatives is the so-called structured reactor, in which a structured substrate is coated with zeolite. Lower pressure drop, shorter diffusional distances and higher geometric surfaces are the principal characteristics of these structured reactors in comparison to conventional fixed bed reactor processes [3,4]. The developments of zeolite coatings for structured reactors have been aided by the advances experienced in recent years concerning the development of zeolite films and membranes [5,6].

In this work, cordierite monolith was chosen as the structured substrate and mordenite as the zeolite coating. Coating by mordenite films was achieved via seeded hydrothermal synthesis and cobalt was incorporated into the mordenite layer by cationic exchange. The main goal of this work was to study the distribution of the different elements along the zeolite coating and the zeolite–cordierite interface, as well as to analyze the different cobalt species and their effects on the catalytic activity for NO selective catalytic reduction (SCR) with methane.

2. Experimental

2.1. Hydrothermal synthesis of mordenite onto cordierite monolith (Na-Mor/Cor)

Cordierite ($2MgO–2Al_2O_3–5SiO_2$) monoliths (Corning, 400 cells in^{-2}, 0.1 mm average wall thickness) were used as

* Corresponding authors.
E-mail addresses: mulla@fiqus.unl.edu.ar (M.A. Ulla), Jesus.Santamaria@unizar.es (J. Santamaría).

0920-5861/$ – see front matter © 2007 Elsevier B.V. All rights reserved.
doi:10.1016/j.cattod.2007.11.052

substrates, from which 1 cm × 1 cm × 2 cm representative samples were cut. The growth of mordenite onto the substrate was carried out via hydrothermal synthesis after seeding the substrate walls. A dip-coating procedure was used for seeding the cordierite substrate. A suspension of commercial mordenite seeds (Tosoh Co., Si/Al: 5.1) with a concentration of 20 g l^{-1} was prepared and then the substrate was dipped in the suspension and dried at room temperature for 1 h; the procedure was repeated three times.

Before synthesis, the substrates were wrapped with Teflon tape on the outer part, fixed to a Teflon holder and placed vertically with their channels aligned parallel to the main axis of the autoclave. The Teflon holder was then filled with the gel solution (molar composition: H_2O:SiO_2:Na_2O:Al_2O_3 = 80:1:0.38:0.025) and placed in a convection oven at 180 °C for 24 h. After synthesis, the substrates were rinsed with distilled water, washed in an ultrasonic bath for 10 min, to remove any loosely adhering material, and then dried in a furnace at 110 °C for 12 h. Further details of the synthesis procedure are presented in Ref. [4].

2.2. Incorporation of Co into the mordenite layer

The mordenite coatings obtained were in the sodium form (Na-MOR/Cor). One of them was converted to the ammonium form via cationic exchange procedure using a 1 M solution of NH_4NO_3 at 80 °C for 24 h, and then dried at 120 °C for 8 h (H-MOR/Cor).

Co incorporation was accomplished in both type of samples (Na-MOR/Cor and H-MOR/Cor) by cationic exchange using a solution of $Co(CH_3COO)_2$ (0.025 M). The ratio of solution volume to zeolite weight was 10 ml g^{-1}. The cation exchange procedure was carried out at 25 °C for 16 h and then during 4 h at 60 °C or 80 °C. These two final temperatures were selected to produce different ion exchange extent. For the sample named Co,Na-MOR/Cor(80), the final temperature was 80 °C whereas for Co,Na-MOR/Cor(60) and Co,H-MOR/Cor(60) was 60 °C.

All the samples were then calcined following the standard calcination procedure: heated under a flow of diluted oxygen at 5 °C min^{-1} up to 400 °C, then maintained at temperature for 8 h.

2.3. Morphological and physicochemical characterization

The surface and cross-section of mordenite coating onto the cordierite monolith were examined by scanning electron microscopy (SEM, JEOL JSM 6400) operated at 20 kV. The different component (Al, Si, Mg, and Co) profiles were measured using an energy-dispersive X-ray analysis (EDX) system attached to the SEM instrument. X-ray diffraction patterns of the different samples were obtained with a diffractometer using the Cu Kα radiation (Rigaku/Max System). The mordenite coating adhesion was evaluated using ultrasonic procedure followed by Zamaro et al. [7].

The temperature-programmed reduction (TPR) experiments were performed in an Okhura TP-2002S instrument whereas the NO_x temperature-programmed desorption (NO_x-TPD) experiments were carried out in the same continuous flow system used for catalytic tests. In this case, the adsorption stream contained 10% NO in He for 15 min at 25 °C. The reversibly adsorbed NO was removed by sweeping with He at room temperature. The sample was then heated in He flow, at a rate of 10 °C min^{-1}. The desorbed NO_x species were analyzed by IR spectroscopy.

2.4. Catalytic tests

The selective catalytic reduction of NO with CH_4 in oxygen excess was performed as a test reaction in a continuous flow system under atmospheric pressure at temperatures between 350 °C and 550 °C. The typical composition of the reacting stream was: 1000 ppm NO, 1000 ppm CH_4 and 2% O_2 in He (GHSV = 6500 h^{-1} referred to zeolite weight or GHVV = 5000 h^{-1} referred to the substrate volume). The gaseous composition of the reactor effluent was monitored for CH_4, CO, NO, N_2O and NO_2 using a Fourier transform infrared spectrometer (FTIR), Thermo Matson Genesis II, equipped with a gas IR cell, having a 15 cm path length (47 ml volume). A total of 100 scans were collected with a nominal resolution of 1 cm^{-1}. Five spectra were recorded at each of the selected reaction temperatures. The first spectrum was recorded after 40 min on stream to assure that steady-state activity had been reached. Besides, the produced nitrogen was monitored by on-line gas chromatography, which allows corroborating the balance of nitrogen compounds.

The CH_4 and the NO to N_2 conversions were defined as

$$X_{CH_4} = \frac{([CH_4]^\circ - [CH_4]) \times 100}{[CH_4]^\circ},$$

$$X_{NO\ to\ N_2} = \frac{([NO]^\circ - ([NO] + [NO_2])) \times 100}{[NO]^\circ}$$

The $[CH_4]^\circ$ and the $[NO]^\circ$ stand for the CH_4 and the NO concentration of the feed, respectively.

3. Results and discussion

3.1. Mordenite coating characterization

The zeolite grown covered the entire surface of the cordierite monolith as shown in Fig. 1a and b. The coating thickness varied between 30 μm and 100 μm, and the average weight gain was 40%. The ratio between the substrate weight and the synthesis gel volume used is the main factor in controlling the ratio of synthesis of mordenite crystals on the cordierite walls versus homogeneous synthesis within the gel [4]. The zeolite crystal showed needle-like shape with micrometric dimensions. In addition, the mordenite film was largely free of intergrowth between crystals thereby maintaining crystal individuality, which facilitates access from the fluid phase [4]. The XRD patterns of the samples (not shown) confirmed the formation of mordenite coating as the only zeolite phase present. However, some SEM micrographs indicated the presence of isolated crystals with analcime (a zeolite-type structure with a Si/Al ratio around 2) morphology (Fig. 2). In spite of this, the concentration of analcime crystals must have been very low, as

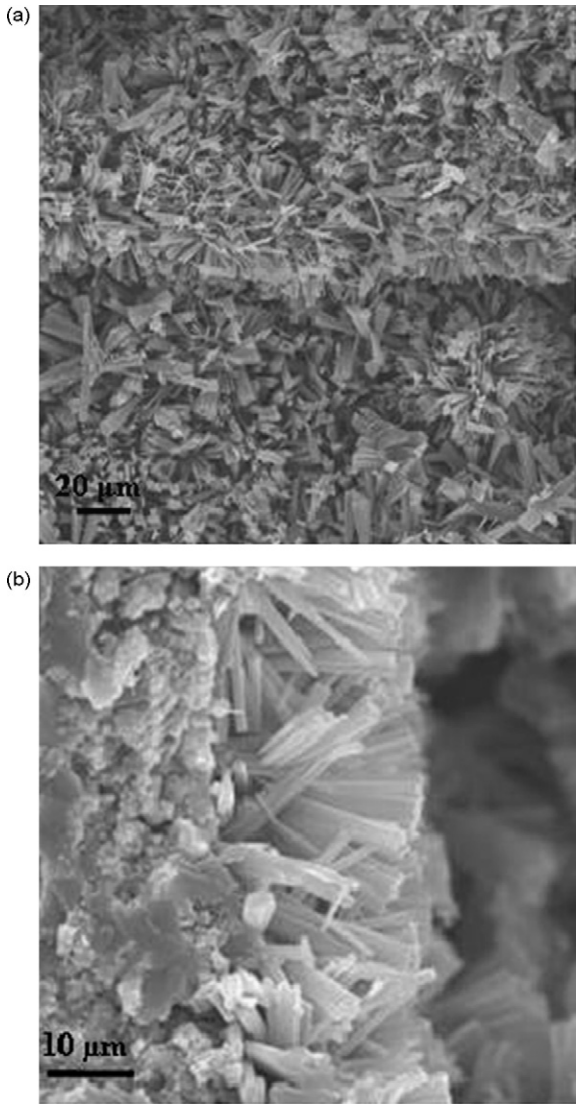

Fig. 1. Morphology of mordenite coating onto cordierite monolith: (a) top view and (b) cross-section.

no peaks corresponding to this structure were observed in the XRD patterns. In the case of Co,Na-MOR/Cor(80) the ANA crystals were not detected in the electron microscope observation.

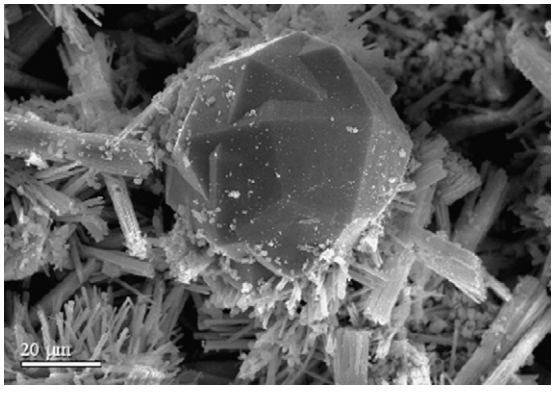

Fig. 2. Isolated analcime crystal onto the surface of the Na-MOR/Cor monolith.

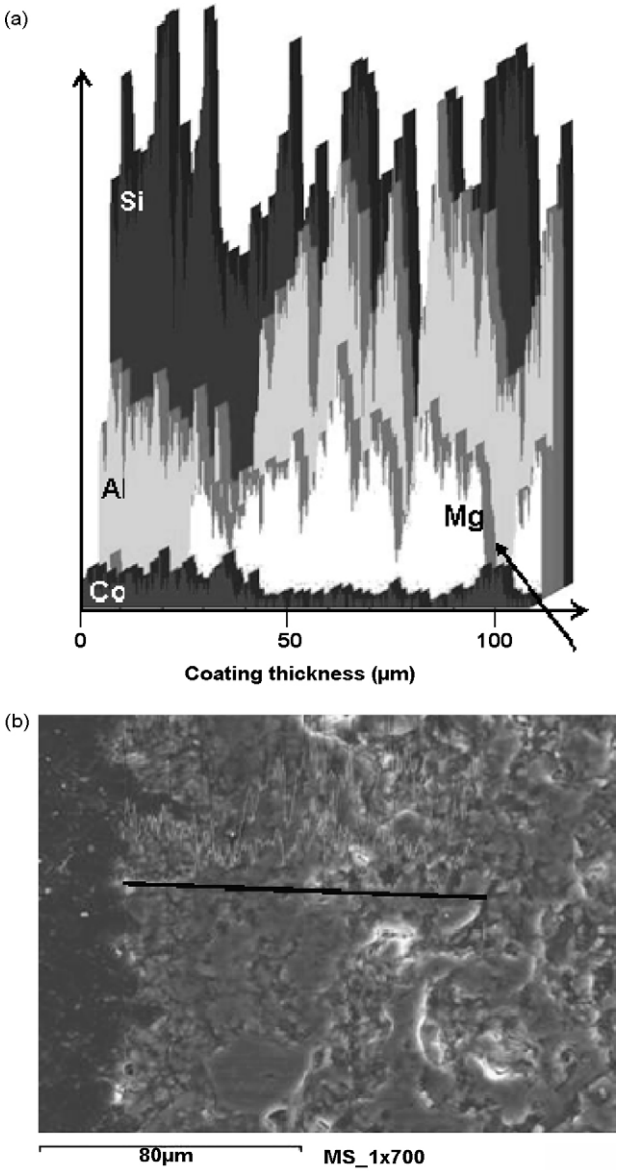

Fig. 3. (a) EDX composition profile of Al, Si, Mg and Co for the Co,Na-Mor/Cor(60) and (b) SEM micrograph of the analyzed area. The black line corresponds to the sampling track.

The adhesion of the mordenite to the cordierite walls was confirmed via the ultrasonic procedure proposed by Zamaro et al. [7]; the weight lost during 1 h ultrasonic treatment was less than 0.1%.

The atomic concentration profiles for Si, Al, Mg and Co across the mordenite coating are presented in Fig. 3a. The SEM micrograph of the analyzed area is included (Fig. 3b, where the line represents the sampling track). The M/Al ratios (M = Si or Co) for each of the prepared samples, along the initial 10 μm of the coating (from top of the layer to the support) are presented in Table 1.

The Si/Al ratio in the mordenite layer varied between 5 and 8 whereas this ratio in the cordierite layer was around 1.25. Therefore, it was possible to identify the mordenite–cordierite interface through the differences in intensities of Al and Si (Fig. 3a). In addition, the Mg profile also shows a strong shift at

Table 1
M/Al ratio (M = Si, Co) at different positions (0 μm corresponds to the top edge of the zeolite layer) on the Co-mordenite coating (EDX)

Structured catalysts	Position (μm)	Si/Al	Co/Al
Co,Na-MOR/Cor(80)	0	7.90	0.35
	5	8.00	0.36
	10	7.88	0.36
Co,Na-MOR/Cor(60)	0	5.21	0.26
	5	6.23	0.25
	10	7.00	0.24
Co,H-MOR/Cor(60)	0	7.11	0.09
	5	5.00	0.10
	10	5.30	0.09

the interface zone, an expected result since the cordierite structure contains Mg. Since no magnesium was detected in the mordenite coating it can be concluded that no Mg migration from the cordierite to the mordenite occurred during the synthesis procedure.

The elemental profiles presented peaks and valleys (Fig. 3a) indicative of voids in the sampling track that correspond to voids between the zeolite crystals and defects in the cordierite support. These defects could readily be identified in an optical microscopy examination of the initial cordierite monolith (not shown). A closer SEM examination after mordenite growth reveals that mordenite crystals were also synthesized within the macropores of the cordierite support; this is shown in Fig. 3a (pointed out with an arrow), at a location were no Mg appears and the Si/Al ratio corresponds to the zeolite value.

The Si/Al ratio of the mordenite coating, for all the samples prepared, was lower than the ratio in the synthesis gel (Si/Al = 20) suggesting that to some extent Al from the cordierite could be incorporated to the mordenite coating during the synthesis. Besides, this ratio for Co,Na-MOR/Cor(80) was around 8 while for Co,Na-MOR/Cor(60) and Co,H-MOR/Cor(60) was slightly lower with some scattering (Table 1). These differences reveal the different extent of Al leaching depending on the synthesis conditions.

A homogeneous Co/Al ratio, across the mordenite layers, was observed for the three samples (Table 1). The Co loadings of Co,Na-MOR/Cor samples depended on the final temperature used during the ion-exchange procedure, as it was expected a lower temperature, corresponds to a lower Co loading. Concerning the Co,H-MOR/Cor(60) sample, in which the exchange procedure was done using the ammonium form mordenite, the amount of Co loading was noticeably lower (Table 1).

3.2. Distribution of Co species in the mordenite coatings

The reducibility of Co in Co-exchanged zeolites seems well established, as well as the peak assignments to different Co species that allow monitoring of the process [8–10]. Therefore temperature-programmed reduction was used to identify the different Co species present in the Co-MOR/Cor samples.

The temperature-programmed reduction profiles for Co,Na-MOR/Cor(80) fresh and after catalytic reaction are shown in Fig. 4; comparing both curves, no significant changes were

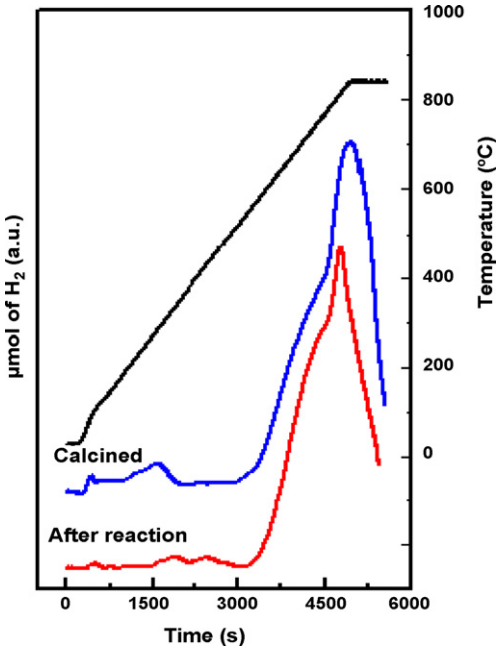

Fig. 4. Temperature-programmed reduction analysis of Co,Na-Mor/Cor(80) sample.

noticed. The peak at high temperature (about 820 °C) was associated to the reduction of Co^{2+} located in exchange sites belonging to the mordenite structure, whereas the shoulder around 600 °C was attributed to the reducibility of hydro-Co species and highly dispersed CoO_x. Hydrogen consumption in the temperature range of 250–450 °C was assigned to Co_3O_4 spinel reduction [8–10].

The distribution of cobalt cations located at different exchange sites of the mordenite structure can be identified by analyzing the NO adsorption. The characteristic interactions of NO adsorbed on these Co sites are well known [11,12]. The fraction of Co^{2+} located at exchange sites in the mordenite main channels (α sites) adsorbs this molecule preferably as dinitrosyl (Co–$(NO)_2$) while mononitrosyl is adsorbed on those exchanged Co^{2+} placed near the site pocket of the mordenite structure (β sites) [11]. Thus, if all of the cobalt loaded in each sample was as Co^{2+} in exchange sites, the NO/Co ratio should be between 1 and 2. The NO_x-TPD results for Na containing samples, Co,Na-MOR/Cor(60) and Co,Na-MOR/Cor(80), indicated that their the NO/Co ratio was 0.23 and 0.54, respectively. These ratios, lower than the expected value, would be associated to the highly dispersed CoO_x, hydroxo-Co species and some Co_3O_4, whose presence was confirmed by the TPR experiments (Fig. 3). The existence of these Co species would decrease the number of exposed cobalt and therefore the number of NO adsorption sites, In addition, the possible obstruction of mordenite micropores by these Co species hindering the NO accessibility to the channels should also be considered. The Co,Na-MOR/Cor(60) sample has lower NO/Co ratio than the Co,Na-MOR/Cor(80) sample, suggesting that the Co^{2+} exchanged in the latter sample is higher.

The NO/Co ratio for Co,H-MOR/Cor(60) was 0.8 (Table 2) but the Co loading of this sample was rather low, Co/Al = 0.1.

Table 2
Quantification of desorbed NO_x (NO_x-TPD)

Structured catalyst	Co Al	NO_x Co	NO (μmol g^{-1})	NO_2 (T_{MAX}) (μmol g^{-1})
Co,Na-MOR/Cor(80)	0.35	0.55	116.7	19.7 (400 °C)
Co,Na-MOR/Cor(60)	0.25	0.23	29.8	8.9 (360 °C)
Co,H-MOR/Cor(60)	0.10	0.8	41.1	20.8 (365 °C)

Kaucký et al. [11] reported that for Co-mordenite with low exchange Co level, the β sites are the preferred sites to be exchanged. Therefore, it was expected that Co was placed at β sites for Co,H-MOR/Cor(60) and taking into account that the NO molecule adsorbs as mononitrosyl in this kind of sites, the NO/Co ratio = 0.8 obtained for this sample suggested that the main Co species in this sample would be Co^{2+} in exchange position, β site.

The NO_x-TPD profiles for the three samples were quite similar, Fig. 5 corresponds to the Co, Na-MOR(80)/Cor sample. Three different peaks could be observed:

(i) A main asymmetric desorption peak at 150 °C, indicating that at least two different Co exchanged sites were interacting with NO molecules [12].
(ii) A NO_2 peak at 350–400 °C, which could be attributed to the reaction of NO and surface oxygen. In spite of the NO disproportion reaction to NO_2 and N_2O could also take place, this reaction appeared not to turn out since the N_2O was not detected during the desorption process.

The quantification of the NO_2 produced per gram of solid for the three Co-mordenite samples is shown in Table 2. Comparing this value for the Na containing catalysts was inferred that the amount of NO_2 desorbed is lower for the sample with low Co/Al ratio (Co,Na-MOR/Cor(60)). As it was mentioned before, this sample had high concentration of cobalt species different from Co^{2+} exchanged, such as highly dispersed CoO_x, hydroxo-Co and Co_3O_4, therefore no link between the NO_2 produced and these Co species could be assigned.On the other hand, rather similar values of the amount of NO_2 desorbed for Co,Na-MOR/Cor(80) and Co,H-MOR/Cor(60) were obtained even though, their Co species, Co exchange sites, and their NO/Co ratio were significantly different. These results agree well with a scenario where NO and surface oxygen react to produce NO_2.

(iii) The sample with high Co loading, Co,Na-MOR/Cor(80), had a second large desorption peak of NO at 450 °C. This extra signal was characteristic of Co-mordenite coating onto cordierite monolith since this was absent on the NO_x-TPD profiles of the Co-mordenite powder [10]. Therefore, the NO desorption at high temperature would be attributed to Co^{2+} exchange sites more hindered such as those of mordenite grown in cordierite wall macropores (Fig. 3a) and those at the core of large mordenite crystals.

3.3. Relation between catalytic activity and distribution of the different Co species

Figs. 6–8 show the catalytic behavior for NO-SCR with CH_4 in O_2 excess for the three prepared structured catalysts.

In case of Na containing catalysts, Co,Na-MOR/Cor(80) and Co,Na-MOR/Cor(60), the NO conversion to N_2 increased with the temperature up to 450 °C and then declined, while the methane conversion continued increasing until almost complete conversion was reached. This behavior is typical for NO-SCR with methane over Co-mordenite powder [13]. A reasonable

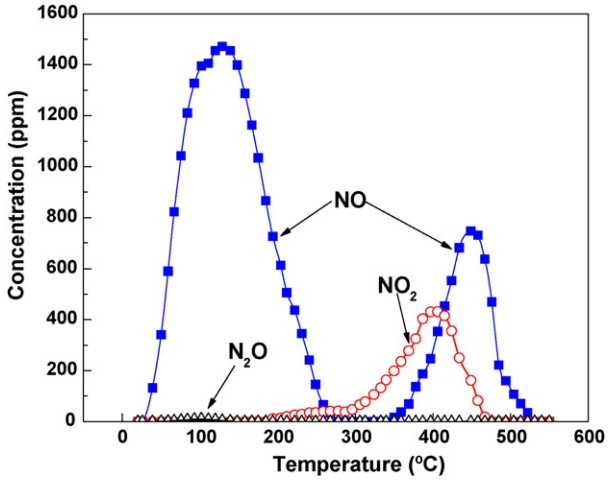

Fig. 5. Temperature-programmed desorption of NO. Co,Na-Mor/Cor(80) sample.

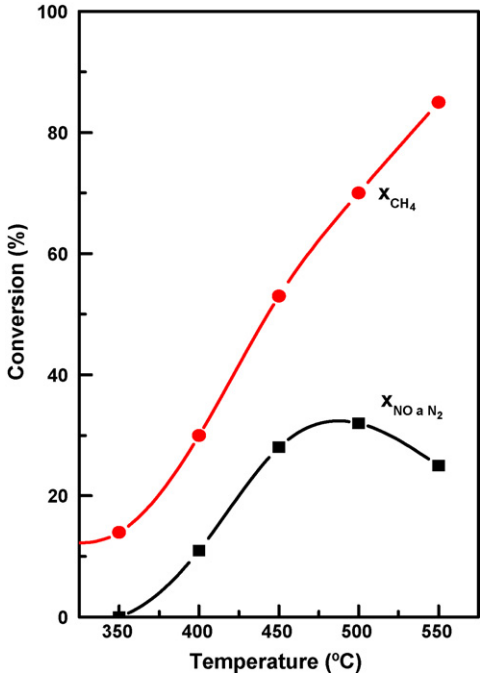

Fig. 6. Catalytic activity for NO-SCR with CH_4 in excess of oxygen over Co,Na-MOR/Cor(80). Reaction conditions: 1000 ppm NO, 1000 ppm CH_4, 2% O_2 in He and GHSV = 6500 h^{-1} referred to zeolite weight.

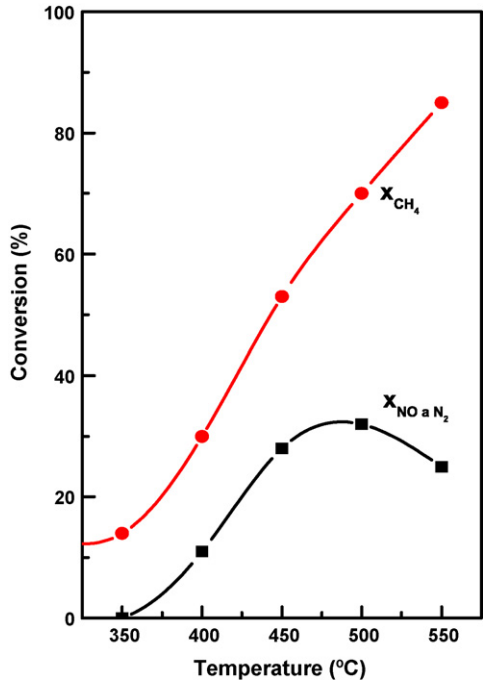

Fig. 7. Catalytic activity for NO-SCR with CH_4 in excess of oxygen over Co,Na-Mor/Cor(60). Reaction conditions: 1000 ppm NO, 1000 ppm CH_4, 2% O_2 in He and GHSV = 6500 h^{-1} referred to zeolite weight.

explanation follows from the analysis of the following reactions taking place during the catalytic evaluation test:

$$CH_4 + 2NO + O_2 \rightarrow N_2 + CO_2 + 2H_2O \quad (1)$$

$$NO + O_2 \rightarrow NO_2 \quad (2)$$

$$CH_4 + 2O_2 \rightarrow CO_2 + 2H_2O \quad (3)$$

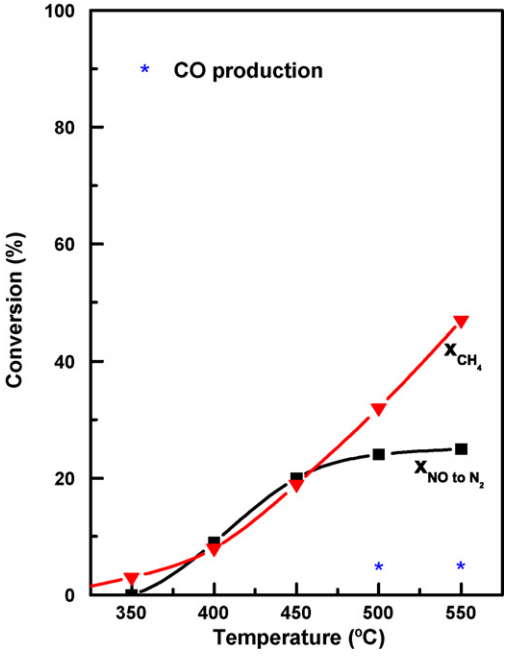

Fig. 8. Catalytic activity for NO-SCR with CH_4 in excess of oxygen over Co,H-Mor/Cor(60). Reaction conditions: 1000 ppm NO, 1000 ppm CH_4, 2% O_2 in He and GHSV = 6500 h^{-1} referred to zeolite weight.

At high temperatures, NO oxidation (reaction (2)) becomes thermodynamically limited and reaction (3) prevails over the SCR of NO with methane (reaction (1)). This means that methane, a necessary reactant for reactions (1) and (3) becomes rapidly consumed by reaction (3) at higher temperatures. This limits the extension of reaction (1), and as a consequence a maximum appears in the curve representing the amount of NO converted to N_2 with temperature.

The lower activity observed for the Co,Na-MOR/Cor(60) catalyst was consistent with its lower Co loading and its lower NO/Co ratio determined by the NO-TPD experiments. The active sites for this reaction on Co-mordenite are associated to exchange Co^{2+} sites accessible to the reactants [11]. According to the NO desorption and the Co/Al ratio, the protonic sample, Co,H-MOR/Cor(60), exhibited most of the cobalt loading as Co^{2+} exchange in β site, which is considered an active site, but with less accessibility to the reactants compared to α site located in the main mordenite channel. Moreover, the amount of β sites occupied by cobalt appeared to be small because of the low Co/Al ratio of this sample. Therefore the protonic catalyst contained a low active site concentration and with moderate accessibility. This analysis was consistent with the catalytic behavior observed: low conversion of NO and CH_4 along the temperature range tested (Fig. 8), at 550 °C the methane conversion was just close to 50% and CO also was detected as a product.

4. Conclusions

- Well-crystallized mordenite coatings were obtained on cordierite monoliths with a high zeolite loading after a 24 h hydrothermal synthesis process. Crystals developed needle-type shapes with micrometric dimensions and in most of the cases, their individuality was maintained. The presence of isolated analcime crystals was also found by SEM but not by XRD, due to their presence in low concentrations.
- The Si/Al ratio determined across the mordenite coating was lower than that of synthesis gel (Si/Al = 20) suggesting that Al transfer from cordierite walls to the zeolite layer takes place during the synthesis procedure; however, this transfer was not found relevant for the other cordierite component (Mg).
- The Co/Al ratio was homogeneous through the mordenite layer for the three structured catalysts. However, different ratios were obtained in each sample depending upon the cationic exchange conditions used.
- The mordenite growth also occurred in the macropores of cordierite walls and the Co exchange took place even in those areas.
- The cobalt species present were mainly Co^{2+} in exchange positions, hydroxo-Co and highly dispersed CoO_x, it was also possible to detect a small amount corresponding to the Co_3O_4 spinel. Those Co species different from exchanged Co^{2+} would decrease the proportion of Co, which is able to interact with NO molecules. Besides, they also could hinder access to the mordenite channels, diminishing the NO accessibility. Both circumstances led to NO/Co ratio < 1.

- The NO_x desorption profiles suggested that at least two different Co exchange sites were present and some oxygen remained on the surface after calcination. The NO signal at 450 °C, characteristic of the Co-mordenite coating, would be attributed to Co^{2+}exchange sites with low accessibility such as those of mordenite grown into the cordierite macropores and those at the core of large mordenite crystals.
- Co-mordenite coating onto cordierite monoliths presented a catalytic performance for NO-SCR with methane, which was comparable to that of Co-mordenite powder. The active sites for this reaction are associated to Co^{2+} exchange sites accessible to the reactants.

Acknowledgements

The authors wish to acknowledge the financial support received from MEC-DGCYT (Spain), ANPCyT-UNL (Argentina), Banco RIO-UNIVERSIA 2004 and AECI-PIC 2006 program.

References

[1] M. Stöcker, Micropor. Mesopor. Mater. 82 (2005) 157.
[2] G. Winé, J.P. Tessionner, S. Rigolet, C. Marichal, M.J. Ledoux, C. Pham-Huu, Appl. Catal. 248 (2005) 113.
[3] M. Heck, R. Ferrauto, In Catalytic Air Pollution Control Commercial Technology, Van Nostrand, Reinhold, 1995.
[4] M.A. Ulla, R. Mallada, J. Coronas, E.E. Miró, J. Santamaría, Chem. Commun. (2004) 528.
[5] J. Coronas, J. Santamaria, Top. Catal. 29 (2004) 29.
[6] J. Coronas, J. Santamaría, Chem. Eng. Sci. 59 (2004) 4789.
[7] J.M. Zamaro, M.A. Ulla, E.E. Miró, Chem. Eng. J. 106 (2005) 25.
[8] l. Gutierrez, E.A. Lombardo, J.O. Petunchi, Appl. Catal. A 194–195 (2000) 169.
[9] C. Resini, T. Montanari, G. Bagnasco, M. Turco, G. Busca, F. Bregani, M. Notaro, G. Rocchini, J. Catal. 214 (2003) 179.
[10] M.A. Ulla, L. Gutierrez, E.A. Lombardo, F. Lónyi, J. Valyon, Appl. Catal. A 277 (2004) 227.
[11] D. Kaucký, A. Vandrová, J. Dedecek, B. Wichterlová, J. Catal. 194 (2000) 318.
[12] W.-X. Zhang, H. Yahiro, M. Iwamoto, J. Chem. Soc., Faraday Trans. 91 (1995) 767.
[13] L. Gutierrez, A. Boix, J. Petunchi, J. Catal. 179 (1998) 179.